Click Here for Full Article

South Pacific hotspot swells dynamically supported by mantle flows

Claudia Adam,[1,2] Masaki Yoshida,[1] Takehi Isse,[3] Daisuke Suetsugu,[1] Yoshio Fukao,[1] and Guilhem Barruol[4]

[1] The dynamics of mantle plumes and the origin of their associated swells remain some of the most controversial topics in geodynamics. Here we construct a numerical model of the mantle flow beneath the French Polynesia region. Our study is based on a new regional seismic tomography model, which high resolution allows obtaining information at the scale of plumes. We find excellent correlations between the observed and the modeled dynamic swells, between the modeled flow pattern and the active volcanism and between the buoyancy fluxes obtained from our numerical model and the ones deduced from the swells morphology. These outstanding fits reveal for the first time that a direct link exists between the surface observations and mantle flows. **Citation:** Adam, C., M. Yoshida, T. Isse, D. Suetsugu, Y. Fukao, and G. Barruol (2010), South Pacific hotspot swells dynamically supported by mantle flows, *Geophys. Res. Lett.*, *37*, L08302, doi:10.1029/2010GL042534.

1. Introduction

[2] According to the plume theory, originally proposed by *Morgan* [1968], the hotspot volcanoes are created by jets of hot material (plumes) rising from the deep mantle. With later studies, troubling inconsistencies began to emerge and other phenomena are invoked to explain intraplate volcanism [e.g., *McNutt et al.*, 1997; *Hirano et al.*, 2006], thus tending to nail the plume coffin [*McNutt*, 2006; *Hofmann and Hart*, 2007]. However, the problems encountered may simply be "the maturing of a valid theory to deal with the complexity of the real planet" [*McNutt*, 2006]. This alternative is tested here by studying the dynamics of the South Pacific plumes through a new numerical model of mantle flow based on a highly-resolved seismic tomography model.

[3] Our study focuses on French Polynesia, a region characterized by the highest concentration of hotspot volcanism. The rate of volcanism is indeed 3–4 times greater than in the other oceans and 14% of the active hotspots of the earth are concentrated in an area covering less than 5% of the globe. We find a wide range of volcanic features like en-echelon ridges, isolated seamounts and five chains of mid-plate volcanoes: the Society, the Marquesas, the Tuamotu, Pitcairn-Gambier and the Cook-Austral (Figure 1a).

The mechanisms responsible for loading of these chains, and the origin of the associated swells are still under debate [*McNutt et al.*, 1997; *Jordahl et al.*, 2004; *Monnereau and Cazenave*, 1990; *McNutt*, 1988; *Crough*, 1978]. In order to bring new insights on these topics, we calculate the instantaneous mantle flow by using a new, highly resolved seismic tomography model.

2. Model

[4] The shear wave tomography model is obtained through the inversion of Rayleigh waves (see auxiliary material) [see *Isse et al.*, 2006; *Suetsugu et al.*, 2009], registered at two new networks of broad band seismic stations, deployed on the seafloor [*Suetsugu et al.*, 2005] and on the islands [*Barruol et al.*, 2002].[1] For shallow depths (0–240km), slow anomalies are found in the vicinity of the South Pacific hot spots, which could represent narrow plumes in the upper mantle [*Isse et al.*, 2006]. The Society, Macdonald and Pitcairn hot spots appear however, to be rooted at depths greater than 240 km [*Suetsugu et al.*, 2009].

[5] We convert the seismic velocity anomalies (δv) into density anomalies ($\delta \rho$) with a conversion factor $R_{\rho/vs}(= \delta \rho / \delta v_s)$ of 0.17 (Figure 1b and auxiliary material). We then compute the instantaneous mantle flow driven by the density anomalies by solving the conservation equations of mass and momentum in a regional three-dimensional spherical shell geometry. The computation domain extends between latitudes 0 and 32°S, longitudes 174 and 232°E, and depths 0–240 km. Following the work of *Yoshida* [2008], we used the finite volume method for the discretization of the basic equations (see auxiliary material). We impose a viscosity profile which describes a highly viscous lithosphere (10^{23} Pas between depths 0 and 30 km) overlying a low viscosity asthenosphere (10^{20} Pas between depths 30 and 240 km). The impermeable and shear stress-free conditions are adopted on the top (0 km depth) and bottom (240 km depth) surface boundaries. The flows across lateral boundaries are taken to be symmetric. Once we obtain the velocity and pressure fields, representative of the convection driven by the density anomalies within the whole model domain, we estimate the dynamic topography at the top surface boundary (see auxiliary material).

3. Hotspot Swells and Dynamic Topography

[6] The dynamic topography is presented in Figure 2c. We notice a good overall correlation between the observed (Figures 2a and 2b) and the modelled swells, in spite the fact

[1]Institute for Research on Earth Evolution, Japan Agency for Marine-Earth Science and Technology, Yokosuka, Japan.
[2]Centro de Geofisica de Évora, Universidade de Évora, Évora, Portugal.
[3]Earthquake Research Institute, Bunkyoku, Tokyo, Japan.
[4]Université de Montpellier II, Montpellier, France.

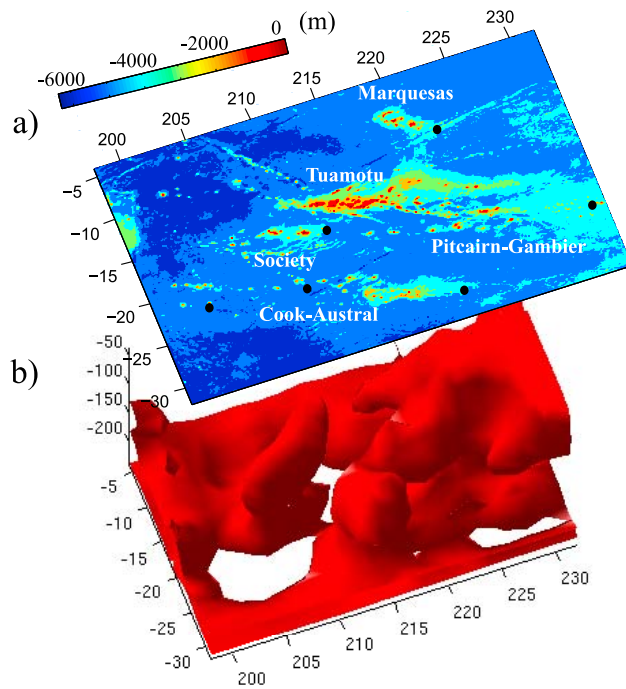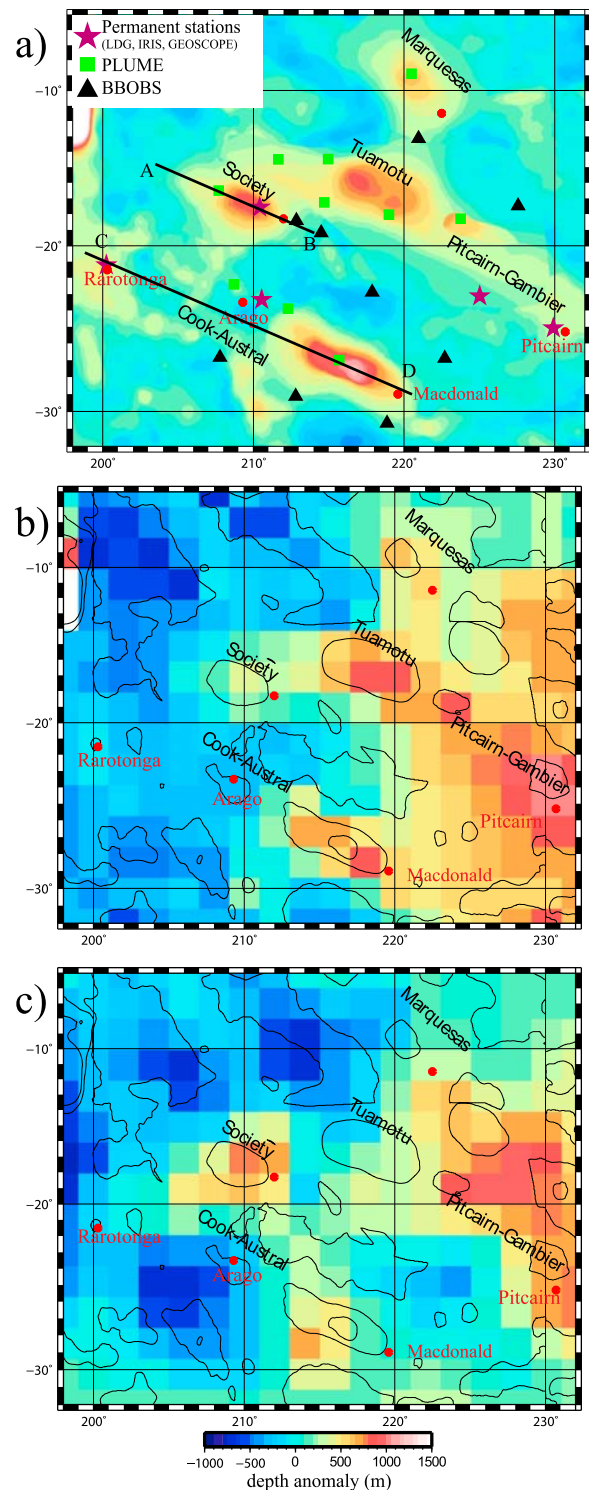[1]Auxiliary materials are available in the HTML. doi:10.1029/2010GL042534.

Figure 1. French Polynesia region. (a) Bathymetry and names of the hotspot chains. The black disks represent the young volcanoes. (b) View of the mantle density anomalies deduced from our tomographic model. The red iso-surface represents the −30 kgm^{-3} density anomaly.

studies demonstrate that most of the volcanism there is produced by non-hotspot processes [*McNutt et al.*, 1997; *Jordahl et al.*, 2004]. Our result demonstrates that, whatever the mechanism responsible for the volcanism emplacement, the buoyant ascent of the mantle plays a major role in the swell morphology.

[7] The dynamic model does not recover the Marquesas and the westernmost part of the Tuamotu swells but it has been shown that these have shallow origins, respectively crustal underplating [*McNutt and Bonneville*, 2000] and a large plateau capped with sediments, limestone and basalt

that they have been obtained from totally independent data (bathymetry and seismic tomograms respectively). The hotspot chains are generally associated with bathymetric highs. Their emplacement, wavelength and amplitude are a priori well recovered by the model, indicating that our modelling reproduces the actual mantle flow. In particular, our model recovers the characteristics of the Society swell, the most classical hotspot chain in our study area. The swell over Pitcairn-Gambier and the circular swell associated with Rarotonga, an isolated active volcano, are also well retrieved by our dynamic model. The good correlation we find between the observed and modelled swell over the Macdonald chain is even more relevant. Indeed, previous

Figure 2. French Polynesia swells. (a) The color map represents the observed swells, determined by the same method that *Adam et al.* [2005] used. The red dots represent the location of active volcanism. The seismic station emplacement is shown by the magenta stars (permanent stations), the green squares (PLUME stations) [*Barruol et al.*, 2002] and the black triangles (BBOBS) [*Suetsugu et al.*, 2005]. The AB and CD profiles are used to make depth cross sections (see Figure 3 and discussion in the text). (b) Observed swells with age correction and 2° × 2° sampling. (c) Dynamic topography obtained through a computation using $R_{\rho/vs} = 0.17$ and a viscosity profile which describes a highly viscous lithosphere (10^{23} Pas between depths 0 and 30 km) overlying a low-viscosity asthenosphere (10^{20} Pas between depths 30 and 240 km). The black lines represent the isocontours of the original swells displayed in Figure 2a.
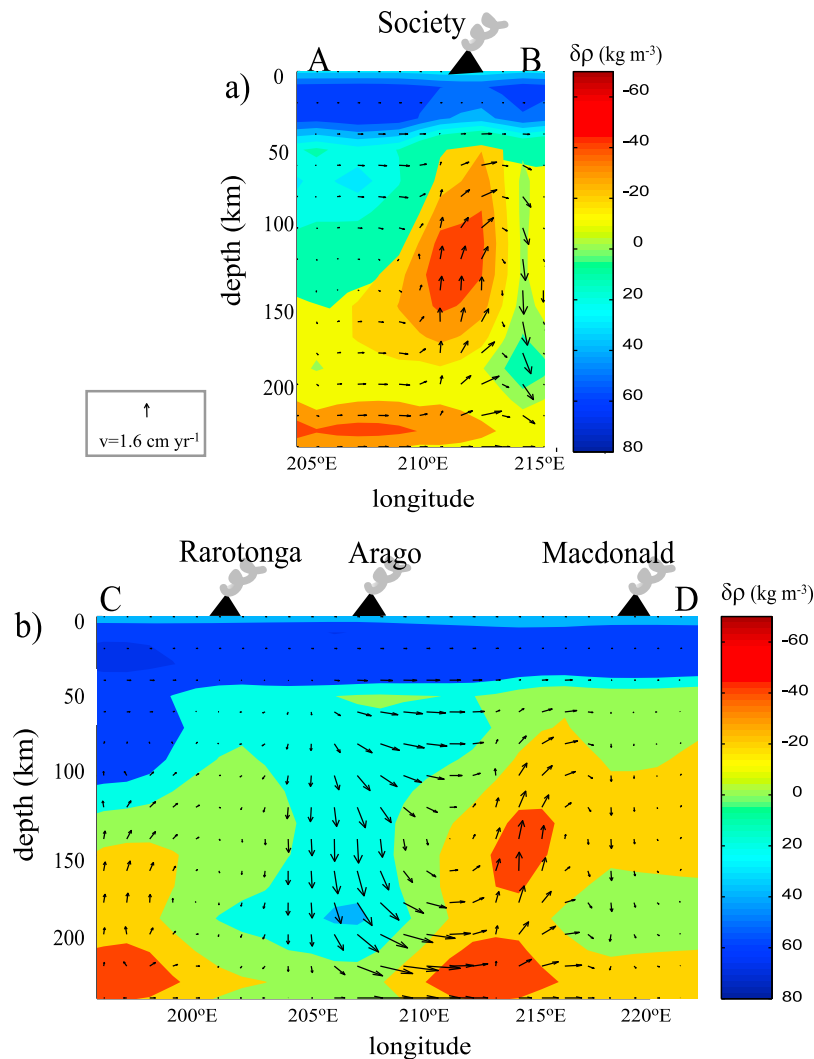
Figure 3. Flow pattern. Depth cross section along the (a) AB and (b) CD profiles displayed in Figure 2a. The color map represents the density anomalies and the arrows the convection driven by them. The schematic volcanoes represent the active volcanism emplacement.

layers [*Ito et al.*, 1995]. However our modelling points out a distinct area of localized upwelling, east of the Tuamotu plateau. Given that no volcanic ages are available, this is the first evidence that the present-day mantle dynamics strongly contributes to the observed depth anomaly.

[8] The model also recovers the observed bathymetric lows such as the one associated with the active Arago volcano, there again with the correct emplacement, wavelength and amplitude. For hotspot chains, the active volcanism is usually explained by the buoyant uplift of a plume, which consequently creates a bathymetric high. Therefore, the fact that the active volcanism observed at Arago is associated with a bathymetric low is very surprising. Further information on the volcanism emplacement are required. They can be obtained by considering the velocity field induced by the density anomalies.

4. Convection Pattern

[9] Our main result concerning the convection pattern is that the volcanism emplacement is not due to a simple vertical ascent of a plume but rather to a complex interaction

between upwelling and downwelling flows. The Society is the only case, in our study area, which corresponds to the definition originally proposed [*Morgan*, 1968; *Sleep*, 1990]. On the depth cross section along the AB profile (Figure 3a), we can see indeed that the buoyant source (negative density anomaly) located under this chain creates a vertical upwelling reaching the lithosphere directly beneath the active volcanism. For all the other chains, the convection pattern is more complex. However, we find that the emplacement of each active volcano can be explained by our modelled flows.

[10] The Cook-Austral chain has often been taken as an example to argue against the plume theory [*McNutt et al.*, 1997; *Jordahl et al.*, 2004]. Many volcanic stages overlap on this chain [*Bonneville et al.*, 2006] and the latest volcanic emplacement is apparently controlled by the stresses left in the lithosphere by previous loadings [*McNutt et al.*, 1997]. On the depth cross section along the CD profile (Figure 3b), a large low density body, deeper than 50 km, creates an upwelling reaching the lithosphere immediately beneath the observed swell maximum, but far from the active volcanism occurring at Macdonald. At the base of the lithosphere the

Table 1. Buoyancy Fluxes Obtained From the Swells (B_{swells}) and From the Dynamic Model (B_{dyn})[a]

Hotspot	B_{swells}(Mgs^{-1})	B_{dyn}(Mgs^{-1})
Society	1.58 ± 0.15*	1.53
Marquesas	1.42*	-
Tuamotu	0.72 ± 0.18	0.53
Rarotonga	0.92 ± 0.09*	0.04
Macdonald	1.10 ± 0.16	0.74
Pitcairn	0.38 ± 0.22	0.22
Arago	−0.38 ± 0.09	−0.23

[a]The values of B_{dyn} with an asterisk have been published by *Adam et al.* [2005]. The others have been obtained in the present study. The values reported for B_{dyn} are obtained through a modelisation considering a highly viscous lithosphere (10^{23} Pas between depths 0 and 30 km) overlying a low-viscosity asthenosphere (10^{20} Pas between depths 30 and 240 km), and a density to velocity heterogeneity ratio $R_{\rho/vs} = 0.17$. The values of B_{dyn} are taken at 150 km depth.

flow becomes horizontal and streams towards the Macdonald. The volcanism emplacement can then be explained by these lateral flows and may be facilitated by the structural discontinuities of the lithosphere, as previously suggested [*McNutt et al.*, 1997; *Jordahl et al.*, 2004]. This study constitutes however the first evidence that the buoyant ascent of the plume plays a major role in the volcanism loading.

[11] Along the CD profile, we can also see that the mantle beneath the Arago active volcano is characterized by densities slightly higher than the surrounding mantle. This explains the observed and modelled bathymetric lows but does not account for the observed active volcanism since the positive density anomalies create downwgoing flows. However, this downwelling current produces lateral tensile stresses near the base of the lithosphere, which may be responsible for crack-associated magma ascent through the lithosphere.

[12] It is worth noticing that, according to the classical definition, plumes should be deep-rooted buoyant mantle upwellings. Here we demonstrate that the convection occurring in the shallowest part of the mantle (0–240 km depths) is sufficient to explain the active volcanism and the observed swells, while the roots of some hotspots are probably located at greater depths, as indicated by a recent tomography model [*Suetsugu et al.*, 2009]. The buoyancy created by these deeper sources is apparently not required

to explain the surface observations. This result may help in providing a new, more realistic definition of the plume concept.

5. Buoyancy Fluxes

[13] Quantitatively, the measure of the plume strength is given by the buoyancy flux, which measures the flux of material from the mantle. The buoyancy flux can be computed through two independent ways, one based on swell morphology (B_{swells}), and the other on the mantle flow (B_{dyn}) (see auxiliary material) [*Sleep*, 1990; *Davies*, 1988]. In this study, B_{dyn} is computed for the first time from a tomography model. The obtained values are displayed in Table 1 and represented in Figure 4. We can see that the results obtained through the two approaches are very consistent. Indeed, both of our B estimations give the same rank ordering of the hotspot strength. From the strongest to the weakest we find the Society, Macdonald, Rarotonga, Tuamotu, Pitcairn and Arago. The Society and Macdonald ones are only the "strong" plumes with $B > 1$Mgs^{-1} [*Courtillot et al.*, 2003]. The fact that the values found through the two independent approaches are consistent for all the French Polynesia hotspots is outstanding. This implies not only that our dynamic model is supported by independent bathymetry data, but also that we can accurately evaluate the material and heat transported by mantle plumes from a careful estimation of the swell morphology. This would help constrain the role that plumes play into the total heat flow on Earth. Using the B_{swells} listed in Table 1, we found that the total buoyancy flux, B_{total}, of the five hotspots (except Marquesas and Arago) is 4.7 Mgs^{-1}. Taking the thermal expansion coefficient $\alpha = 2.0 \times 10^{-5}$ K^{-1} and the specific heat $c_p = 1250$ Jkg^{-1}K^{-1}, the total heat flow is estimated as $Q = B_{total} \, c_p/\alpha = 0.29$ TW [*Davies*, 1999], which accounts for 9% of the total plume heat flow, 3.4 TW [*Sleep*, 1990], and for around 1% of the total heat flow out of the Earth's mantle, 36 TW [*Davies*, 1999].

6. Conclusion

[14] Using a new, regional, highly resolved seismic tomography model, we model the dynamics of the South Pacific plumes and the resulting dynamic topography. We find excellent correlations between the observed and the modeled dynamic swells and between the modeled flow
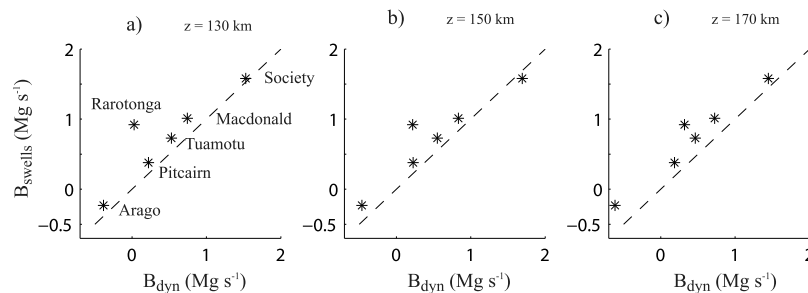

Figure 4. Buoyancy fluxes. The values of the buoyancy fluxes obtained from the observed swells (B_{swell}) are represented as a function of the buoyancy fluxes obtained through the dynamic computation (B_{dyn}) for various depths (130 km, 150 km, and 170 km). We represent the values obtained through a computation using $R_{\rho/vs} = 0.17$ and a viscosity profile which describes a highly viscous lithosphere (10^{23} Pas between depths 0 and 30 km) overlying a low-viscosity asthenosphere (10^{20} Pas between depths 30 and 240 km). The dashed lines represent the $B_{dyn} = B_{swells}$ curve.

pattern and the active volcanism. This demonstrates, for the first time, that a direct link exists between the surface observations and mantle flows. The excellent correlation we find between the buoyancy fluxes obtained from our numerical model and the ones deduced from the swells' morphology has even broader implications. It implies indeed, that we can accurately evaluate the heat transported by mantle plumes from a careful estimation of the swell morphology. We show that the heat transported by the South Pacific plumes accounts for 9% of the total plume heat flux.

References

Adam, C., V. Vidal, and A. Bonneville (2005), MiFil: A method to characterize seafloor swells with application to the south central Pacific, *Geochem. Geophys. Geosyst.*, *6*, Q01003, doi:10.1029/2004GC000814.

Barruol, G., et al. (2002), PLUME investigates South Pacific Superswell, *Eos, Trans. AGU*, *83*(45), 511–514.

Bonneville, A., L. Dosso, and A. Hildenbrand (2006), Temporal Evolution and Geochemical Variability of the South-Pacific Superplume Activity, *Earth Planet. Sci. Lett.*, *244*, 251–269, doi:10.1016/j.epsl.2005.12.037.

Courtillot, V., A. Davaille, B. Besse, and J. Stock (2003), Three distinct types of hotspots in the Earth's mantle, *Earth Planet. Sci. Lett.*, *205*, 295–308.

Crough, S. (1978), Thermal origin of midplate hotspot swells, *Geophys. J. R. Astron. Soc.*, *55*, 451–469.

Davies, G. (1988), Ocean bathymetry and mantle convection. 1. Large-scale flow and hotspots, *J. Geophys. Res.*, *93*(B9), 10,467–10,480.

Davies, G. (1999), *Dynamic Earth: Plates, Plumes and Mantle Convection*, Cambridge Univ. Press, Cambridge, U.K.

Hofmann, A. W., and S. R. Hart (2007), Another nail in which coffin?, *Science*, *315*, 39–40.

Hirano, N., et al. (2006), Volcanism in Response to Plate Flexure, *Science*, *313*, 1426–1428.

Isse, T., D. Suetsugu, H. Shiobara, H. Sugioka, T. Kanazawa, and Y. Fukao (2006), Shear wave speed structure beneath the South Pacific superswell using broadband data from ocean floor and islands, *Geophys. Res. Lett.*, *33*, L16303, doi:10.1029/2006GL026872.

Ito, G., M. McNutt, and R. Gibson (1995), Crustal structure of the Tuamotu Plateau, 15°S and implications for its origin, *J. Geophys. Res.*, *100*, 8097–8114.

Jordahl, K., M. McNutt, and D. Caress (2004), Multiple episodes of volcanism in the Southern Austral Islands: Flexural constraints from bathymetry, seismic reflection, and gravity data, *J. Geophys. Res.*, *109*, B06103, doi:10.1029/2003JB002885.

McNutt, M. (1988), Thermal and mechanical properties of the Cape Verde Rise, *J. Geophys. Res.*, *93*, 2784–2794.

McNutt, M., D. Caress, J. Reynolds, K. Jordahl, and R. Duncan (1997), Failure of plume theory to explain midplate volcanism in the Southern Austral Islands, *Nature*, *389*, 479–482.

McNutt, M., and A. Bonneville (2000), A shallow, chemical origin for the Marquesas swell, *Geochem. Geophys. Geosyst.*, *1*, 1014, doi:10.1029/1999GC000028.

McNutt, M. (2006), Another nail in the plume coffin?, *Science*, *313*, 1394–1395.

Monnereau, M., and A. Cazenave (1990), Depth and geoid anomalies over oceanic hotspot swells: A global survey, *J. Geophys. Res.*, *95*, 15,429–15,438.

Morgan, W. J. (1968), Rises, trenches, great faults, and crustal blocks, *J. Geophys. Res.*, *73*(6), 1959–1982.

Sleep, N. (1990), Hotspots and mantle plumes: Some phenomenology, *J. Geophys. Res.*, *95*(B5), 6715–6736.

Suetsugu, D., et al. (2005), Probing South Pacific mantle plumes with broadband OBS, *Eos, Trans. AGU*, *86*(44), 429–435.

Suetsugu, D., T. Isse, S. Tanaka, M. Obayashi, H. Shiobara, H. Sugioka, T. Kanazawa, Y. Fukao, G. Barruol, D. Reymond, (2009), South Pacific mantle plumes imaged by seismic observation on islands and seafloor, *Geochem. Geophys. Geosyst.*, *10*, Q11014, doi:10.1029/2009GC002533.

Yoshida, M., (2008), Core-mantle boundary topography estimated from numerical simulations of instantaneous mantle flow, *Geochem. Geophys. Geosyst.*, *9*, Q07002, doi:10.1029/2008GC002008.

C. Adam, Y. Fukao, D. Suetsugu, and M. Yoshida, Institute for Research on Earth Evolution, Japan Agency for Marine-Earth Science and Technology, 2-15 Natsushima-cho, Yokosuka, 237-0061, Japan. (adam@uevora.pt)

G. Barruol, Université de Montpellier II, 34095 Montpellier Cedex 5, France.

T. Isse, Earthquake Research Institute, 1-1-1 Yayoi, Bunkyoku, Tokyo, 113-0032, Japan.